Drug target discovery via network modeling: a mathematical model of the *E. coli* folate network response to trimethoprim

Inderpreet Jalli[1¶*], Sophia Lunt[2¶], Wenjia Xu[1&], Carmen Lopez[1&], Andreas Contreras[1&], Cari-Sue Wilmot[3&], Timothy Shih[1&], Frederik Nijhout[1¶]

[1] Department of Biology, Duke University, Durham, North Carolina, United States of America

[2] Department of Biology, Michigan State University, East Lansing, Michigan, United States of America

[3] Department of Earth and Atmospheric Science, University of Houston, Houston, Texas, United States of America

[*]Corresponding author

Email: inderjalli@gmail.com (IJ)

[¶] These members contributed equally to this work.

25 [&] These members also contributed equally to this work.

Abstract

The antibiotic trimethoprim targets the bacterial dihydrofolate reductase enzyme and subsequently affects the entire folate network. We present an expanded mathematical model of trimethoprim's action on the *Escherichia coli* folate network that greatly improves upon Kwon *et al.* (2008). The improvement upon the Kwon Model lends greater insight into the effects of trimethoprim at higher resolution and accuracy. More importantly, the presented mathematical model enables drug target discovery in a way the earlier model could not. Using the improved mathematical model as a scaffold, we use parameter optimization to search for new drug targets that replicate the effect of trimethoprim. We present the model and model-scaffold strategy as an efficient route for drug target discovery.

Introduction

Antibiotic resistance

Antibiotic resistance is a major health policy concern. New and resistant forms of common infections such as tuberculosis necessitate urgent drug development efforts [1-3]. Strategies such as discovering new bacterial communication networks and inhibiting these networks are a popular avenue for drug discovery yet are very expensive in both time and resources. Utilizing math models to gain a greater level of insight into the mechanisms of known drugs may offer opportunities for drug development, using well-studied and richly described pathways that already show weakness to chemical intervention to search for new potential targets [4]. The presented work models the mechanism of a common antibiotic, trimethoprim, at

the biological information layer at which it functions, the metabolic network level. This is done not only to study the mechanism of trimethoprim but to find alternatives to it by attempting to replicate its effect on the folate network, which is known to be critical to cell function. The presented mathematical model improves on previous work by providing a higher resolution model of Trimethoprim's effect on *E. coli*. Without a highly detailed model of the bacterial folate network and trimethoprim's effect on it, the presented strategy of drug target discovery would not be possible.

The folate network and trimethoprim

The folate network is a traditional therapeutic target for both cancerous and bacterial cells due to the integral role folates play in cell division [5, 6]. The folate network provides and accepts one-carbon units for the biosynthesis of amino acids and metabolites such as S-adenosyl methionine (SAM), the universal methyl group donor [7-9]. The antibiotic trimethoprim (TM) inhibits the activity of bacterial dihydrofolate reductase (DHFR), an enzyme that converts dihydrofolate (DHF) to tetrahydrofolate (THF, Fig 1). DHFR inhibition causes a spike in DHF. DHF in turn inhibits folypolyglutamate gamma synthetase (FPGS), the enzyme tasked with adding glutamates to THF and its derivatives [10, 11]. Because folate-catalyzed conversions of one-carbon units are sensitive to glutamation levels of folates, the inhibition of FPGS disrupts critical cell functions [11-14].

Fig 1. A simplistic diagram of effect of trimethoprim on DHFR and FPGS, roughly approximated in Kwon Model.

Boxes = metabolites or antibiotics. Ovals = enzymes, connected to solid lines with arrows indicating metabolite conversions. Dashed lines = inactivation. Trimethoprim inhibits DHFR, which converts DHF_1 to THF_1, leading to a spike in DHF_1. FPGS adds a glutamate to THF_1, and THF_2, converting each to THF_2, and THF_3, respectively.

Folate network models and drug target search

Kwon *et al.* wrote a mathematical model of the disruptive effect of TM focused on folate interconversions which roughly has the structure and resolution of Fig 1, and which we refer to as the *Kwon Model* [10]. The *Kwon Model* compressed all derivatives of THF into three variables, but Kwon et al. recorded experimental data for many THF derivatives. In this work we present a higher resolution version of the *Kwon Model* referred to as the *TM Model,* that exploits the experimental data recorded by Kwon et al. The structure of the *TM Model* is shown in Fig 2. We then use the current *TM Model* as a scaffold for drug target searching by replicating the effects of TM on the *E. coli* folate network without inhibiting DHFR or FPGS. In doing this we create a *Rewired Model* that shows a simulated time-course progression similar to the *TM Model*, but without TM in the simulation. This overall strategy is outlined in Fig 3. The *TM Model* by the nature of its higher resolution, higher number of enzyme and metabolite nodes, and higher accuracy of describing the effect of TM on the folate network, allows for TM alternatives to be explored in a way that the *Kwon Model* cannot. Since multiple interconversions of THF_n and DHF_n are described in the *TM Model*, substituting TM with other possible disruptors of the folate network is feasible, guided by Kwon et al.'s experimental data. This approach allows us to propose new targets for antibiotic activity that would be advantageous against TM-resistant bacteria, and provides a guide for future work on other systems that evolve in response to chemical therapeutics [15, 16].

Fig 2. TM Model of E. coli folate network.

(Ovals = enzymes modeled with Michaelis-Menten equations; boxes = metabolites, TM, or source; dashed lines = inhibitions; straight lines without attached oval = linear conversions. The source (top left)

represents 7,8-dihydropteroate, and mass input is modeled as a linear conversion into DHF_1 only by dihydrofolate synthase (DFHS). Once DHF_1 is produced, it is converted into THF_1 via DHFR. TM inhibits all DHFR activity. THF_1 is converted into THF_2 and then to THF_3 by FPGS, which also works on all THF_n derivatives (except $5MTHF_n$), indicated by thin solid lines. Only FPGS carries out interconversions between glutamation states. All FPGS activities have independent parameter sets. DHF_n inhibits FPGS activity. TS converts $510MTHF_n$ to DHF_n. SHMT converts THF_n to $510MTHF_n$, and MTHFR converts $510mTHF_n$ to $5MTHF_n$. MS does not convert monoglutamates of $5MTHF_n$ to THF_n, but its arrow is shown as other enzymes for simplicity. DHF_n is converted into pAB_n and Pte_n, which act as sinks for the system. Experimental concentration data exists for all metabolites shown in the figure. Pte_n inhibits TS and MS, THF_n inhibits SHMT, and $510MTHF_n$ inhibits MTHFR. These inhibitions however are not as strong as that of TM on DHFR. Formyl THF_n derivatives were not included due to a lack of experimental data.

Fig 3. Drug target searching requires high resolution models.

The Kwon Model is improved upon to create the TM model, which has more metabolite and enzyme nodes. The TM model describes the effects of TM at high resolution and accuracy. The TM model, once developed, is used as a scaffold for drug target searching (Rewired Model). The Kwon Model, due to having only two enzymes (approximated in Fig 1) and compressing all forms of THF into just three nodes, is not viable for drug target discovery (pathway on left).

Abbreviations

Enzymes are listed with abbreviation, name, and Uniprot ID and/or EC number. A subscript indicates the number of glutamates added onto a molecule. Terms such as DHF_n refer to molecules that vary only in number of glutamates. DHFR: dihydrofolate reductase (P0AFS3 / EC: 1.5.1.3), DHFS: dihydrofolate synthase (P08192 / EC: 6.3.2.12), SHMT: serine hydroxymethyltransferase P0A825/ 2.1.2.1), MTHFR: methylenetetrahydrofolate reductase (P42898 / 1.5.1.20), TS: thymidylate synthase (P0A884 / EC: 2.1.1.45), METH: methionine synthase (P13009 / EC: 2.1.1.13), METE/MS: B12 independent methionine synthase (P25665 / EC: 2.1.1.14), FPGS: folypolyglutamate synthetase (P08192 / EC: 6.3.2.17), MET: L-methionine, SAM: S-adenosyl-L-methionine, SRH: S-ribosyl-L-homocysteine, SAH: S-adenosyl-L-homocysteine, HCY: L-homocysteine, TM: trimethoprim, Pte_n: folate glutamate, pABA: para-aminobenzoate,

99 pAB_n: para-aminobenzoylglutamate, DHF_n: dihydrofolate, DHP: dihydropteroic acid, THF_n:
100 tetrahydrofolate, $5MTHF_n$: 5-methyl-THF, $510MTHF_n$: 5,10-methylene-THF. Enzyme parameters
101 are referred to with enzyme abbreviation followed by the type of parameter, then the glutamate
102 that is being acted upon, e.g. DHFRKM1 refers to DHFR's *Km* constant for DHF_1. The included
103 models are heavily focused on the differing activities of enzymes on a variety of unique
104 glutamations of molecules such as THF_n. The velocities of enzymes are denoted by the enzyme
105 abbreviation and then the glutamation level of the general molecule they are named for acting
106 upon. For example, DHFR1 refers to the velocity of DHFR's activity on DHF_1. In the case of FPGS
107 which works on THF_n and its derivatives with differing affinities (except for $5MTHF_n$), the
108 substrate and glutamate are used in the velocity or parameter abbreviation: FPGSTHF1 refers to
109 FPGS activity on the THF_1 substrate. SSE refers to sum of squared errors, a common metric for
110 describing the accuracy of a prediction to the real world data.

111 Materials and Methods

112 Experiments

113 Folate concentrations were measured absolutely as described in Kwon *et al*. [10, 11].
114 Time course progression of folate concentrations and their glutamations can be seen in Fig 4. All
115 rates and velocities are shown in µM/minute. TM was added to *E. coli* growth medium at O.D. ~
116 0.5 at a concentration of 4 µg/mL, immediately after time zero data point collection [10]. *E. coli*
117 strain NCM3722 was used for all experiments [10]. Cells were grown in Gutnick minimal salts
118 medium (Sigma-Aldrich), in a shaking flask at 37°C.

Mathematical modeling of the *TM Model*

All simulations and calculations were carried out in Matlab version 2014a (Simbiology Toolbox), on an Intel Q8200 2.33GHz processor, using Microsoft Windows 7, 64-bit, and ODE solver ode15s. Fig 2 displays the structure of the *TM Model*. Variables are concentrations of DHF_n, pAB_n, Pte_n, THF_n, and all THF_n derivatives, at three glutamation levels. Variable time-course progression is fitted to experimental data shown in Fig 4. The *Kwon Model* summated all THF_n and THF_n derivatives into three variables: THF_1, THF_2, and THF_3. The *Kwon Model* had a lower number of enzyme kinetics equations describing interconversions of DHF_n and THF_n [10]. In the current *TM Model*, THF_n and THF_n derivatives are treated as independent variables, requiring a higher number of detailed enzyme kinetics equations to describe interconversions. This treatment of THF_n derivatives as unique variables allows for high resolution modeling and the creation of the *Rewired Model*. Creating the *Rewired Model* would not be possible at the resolution of the *Kwon Model* because insufficient enzyme nodes exist for a parameter search. Conversion of DHF_n to THF_n by DHFR was modeled by a variant of the Michaelis-Menten equation featuring competitive inhibition:

$$v = \frac{d[P]}{dt} = \frac{V_{max} * [S]}{K_m * \left(1 + \frac{[I]}{K_i}\right) + [S]}$$

Where *Km* is the Michaelis constant, [S] is the concentration of the substrate, K_i is the inhibition constant for TM, [I] is the constant concentration of TM, and *Vmax* is the maximum rate achieved by the enzyme. TM was added to simulations at 40 seconds to reflect experimental protocol. Kwon *et al*. measured a significant reduction of input flux after addition of TM, which is

included in the model unless otherwise stated [10]. If the Michaelis-Menten equation or a variant thereof was not used for a metabolite conversion, a linear rate equation was employed using the form presented below. In the equation below, *Ks* represents a linear transform of the substrate into a product:

$$v = [S] * k_s$$

Fig 4. Folate disruption and simulation of the TM Model.

TM in growth media causes a severe deviation from initial folate concentrations (dots with error bars). THF_n progression shows high similarity to experimental progression (SSE = 1.83, with THF_2 SSE = 1.64). DHF_3 similarity is poor (SSE = 8063), creating bulk of error for model (SSE total = 8947). The experimental time course metabolite concentration data can be found in the data in S3 Table.

Parameters and parameter estimation in the *TM Model*

Parameters are either Michaelis-Menten constants (*Km, Ki, Vmax*) or linear conversion constants (*Ks*). Some parameters are estimated due to insufficient experimental data in published literature, or estimated from an initial data set taken from literature, such as IC_{50} (half maximal inhibitory concentration) values. Estimated parameters were determined by fitting simulations to experimental data via sequential application of the Matlab genetic algorithm and fmincon functions.

Creating the *Rewired Model* to explore alternatives to TM

To find an alternative to TM, we first removed the presence of TM in the *TM Model*. The resultant model with all further modifications is referred to as the *Rewired Model.* We then inserted a set of *in silico* enzyme inhibitors into the *Rewired Model* via parameter modification of existing Michaelis-Menten equations with the aim of creating a simulated time-course folate

concentration progression of the same nature to that caused by TM. The experimental data used to fit the *Rewired Model* was the same as that used for the *TM Model.* DHFR and FPGS were not targeted with *in silico* manipulation in the *Rewired Model* in order to find a true alternative for TM-resistant bacteria. Parameter optimization functions were used to find the proper combination of *in silico* inhibitor. Inhibitors were simulated by introducing alterations of the *Km* and *Vmax* parameters used in the *TM Model*.

Results

Trimethoprim affects polyglutamation – *TM Model*

TM, which is added at 40 seconds into the model simulation, dramatically alters folate pools in the *TM Model* (Fig 4) which replicates the experimental data in *Kwon et al.* with a total SSE of 8948. DHF_3 alone has an SSE of 8063 and is responsible for most of the error. The *TM Model* greatly improves upon the simulation resolution of the *Kwon Model* featured in the same effort [10]. DHF_1 and DHF_2 experience large increases both experimentally and in the *TM Model*. Simulated DHF_3 experiences a minor spike and then slowly stabilizes to near its original concentration instead of showing a drop from initial concentration. A key experimental effect of TM is seen in the model: THF_1 and THF_2 increase after initial drops while THF_3 drops continuously. THF_n derivatives $510mTHF_n$ and $5mTHF_n$ follow similar progressions as seen in experimental data, with the exception of $5mTHF_3$. Fig 5 highlights critical reaction velocities of the *TM Model* to show the drivers of folate concentration progression. Velocity of DHFR1 shows a drop and then a slight rebound, as would be expected due to TM inhibition of DHFR activity. FPGSTHF1 velocity experiences a sudden drop due to an increase in DHF_n which inhibit the

activity of FPGSTHF1. Parameter estimates, drawn from both experimental work and estimation *in silico*, are shown in S1 Table.

Fig 5. Velocities of DHFR, MS on $5MTHF_3$, FPGS on THF_1 and THF_2, under TM.

As expected, velocities drop upon the addition of TM. Some activities such as DHFR on DHF_1 recover slightly over time. Velocity simulations provide reference that assures drivers of simulation mirror biological processes.

Network rewiring to explore TM alternatives – *Rewired Model*

To explore an alternative therapeutic approach to TM, a small number of enzyme inhibitors were added *in silico* while TM was removed, creating the *Rewired Model.* The *Rewired Model*'s parameters were fitted to the same experimental data used to create the *TM Model*. The simulation results of the *Rewired Model* are seen in Fig 6, and the simulated inhibitors are shown in Table 1. The total SSE of the *Rewired Model* as compared to experimental data is 46794, driven mainly by $5mTHF_3$ (SSE = 39929). All THF_n respond as they did in the *TM Model* although not as well *(Rewired Model SSE = 16.41, TM Model SSE = 1.83)*. DHF_n do not follow the *TM Model* pattern, dropping in concentration over the course of the simulation. The proposed inhibitors achieve a partial effect of TM (spiking THF_1 / THF_2, dropping THF_3, alterations of $510mTHF_n$, $5mTHF_n$) without utilizing the DHF spike (further discussion below). *Rewired Model* reaction velocities are shown in S1 Fig. Most velocities except DHFR1 reach steady state early in the *Rewired Model*. In addition, velocities such as FPGSTHF1 increase instead of decreasing as was seen in the *TM Model* (Fig 5).

Fig 6. Rewired Model of E. coli folate to search for new drug targets.

Simulations show an initial disruption of folate concentrations, and then a gradual stabilization. Combined THF_n progression shows high similarity to experimental progression.

Table 1. Inhibitors added in substitution of TM in Rewired Model.

Parameters	*TM Model*	*Rewired Model*	Inhibition Type
MSVM3	1.40E-01	1.00E-02	Noncompetitive
MTHFRKM2	2.99E+00	3.50E+00	Competitive
MTHFRKM3	1.11E-01	1.47E+01	Competitive
SHMTKM3	2.58E+01	6.80E+00	Uncompetitive
SHMTVM3	4.07E+00	3.10E+00	Uncompetitive

Enzymes MS, MTHFR, and SHMT are targeted with noncompetitive, competitive, and uncompetitive inhibitors respectively. TM Model parameters are shown along with inhibition type required to partially recreate effect of TM (spiking THF_1 / THF_2, dropping THF_3, alterations of 510mTHF_n, 5mTHF_n) in Rewired Model.

Discussion

The effect of trimethoprim – *TM Model*

The *TM* Model shows a more accurate and expanded view of the folate network than the previous effort in Kwon *et al*. [10]. SSE scores cannot truly be compared from *TM Model* to *Kwon Model* due to the large increase in metabolites modeled. The explicit addition of TM and THF_n derivatives are the key differences between the *TM Model* and the *Kwon Model*. THF_n derivatives 510mTHF_n and 5mTHF_n were collapsed into THF_n in the *Kwon Model.* In the *TM Model* they are modeled as unique variables as they exist within the bacterial cell and as the experimental data measured them. THF_n and its derivatives are critical to cell functionality due to their connection to the rest of cellular metabolism [8, 9].

The discrete simulation of THF_n and its derivatives allows for accurate modeling of THF_n interconversions to and from its derivative forms. These interconversions feature inhibitory interactions within the network such as Pte_n inhibition of TS. In addition, the inhibition of FPGS by DHF_n can be included, affecting FPGS' activity on THF_n and all its derivatives in varying degrees (Fig 2).

An imbalance of glutamation levels across folates from the zero time point is clearly reflected in the simulation, as it is in the experimental results. The glutamation disruption of THF_n and its derivatives is a critical feature of the *TM Model*. TM operates by disrupting glutamation balance of folates. The spike in DHF_n, shown in the *TM Model*, results in a sudden drop in the velocity of all FPGS activities as seen in Fig 4 and as expected by experiments on FPGS and DHF_n *in vitro* (Kwon et al.). FPGSTHF2 velocity shows a more relaxed response to the DHF_n spike, suggesting some buffering ability in the system.

The poor replication of DHF_3 progression and triple glutamated folates overall is a weakness in the *TM Model.* We suspect it is due to experimental data on enzyme function at triple glutamation being sparse as compared to experimental data on singly glutamated folates. Better descriptions of enzyme function at this glutamation level may allow for better modeling in the future. Most importantly, the increased accuracy of the *TM Model* makes it an excellent platform for drug design.

Network rewiring to explore TM alternatives

The effort to find a TM alternative centered on established drug design principles of using multiple antibiotic agents simultaneously and parameter optimization [17-19]. The simulated

244 inhibitors found via optimization in the *Rewired Model* target MS, MTHFR, and SHMT instead of
245 DHFR alone as seen in Table 1. The overall SSE is driven mainly by inaccuracy in $5mTHF_3$.

246 THF_n follows the progression seen in the *TM Model,* and DHF_n drops in concentration in
247 the *Rewired Model* instead of increasing as it does in the *TM Model*, which is potentially
248 problematic, since DHF_n is a primary driver of the effect of *TM*. However, our objective is to find
249 an alternative and get a disruption in glutamation mix of folates that disrupt cellular metabolism.
250 Our goal is not simply to replicate the domino effect of TM, which causes a spike in DHF_n and
251 then inhibits FPGS. $510mTHF_n$ and $5mTHF_n$ generally (with exception of $5mTHF_3$) follow the same
252 time course progression in the *Rewired Model* as in the *TM Model,* which is encouraging. THF_n
253 and its derivatives are more critical to cell functionality due to their connection to the rest of
254 cellular metabolism [8, 9]. The drop in DHF_n introduces an interesting feature of the *Rewired*
255 *Model.*

256 Despite a poor match to experimental data and the *TM Model* with respect to DHF_n, this
257 proposed set of drug targets may replicate the clinical effect of TM and Sulfamethoxazole.
258 Paradoxically, the drop in DHF_n replicates the task of the drug Sulfamethoxazole, which is used
259 clinically with TM (the target of this drug target search effort). Sulfamethoxazole targets the
260 enzyme DHFS, which synthesizes DHF_1 and therefore inputs mass into the folate network.
261 Sulfamethoxazole and TM clinically work together to fully shut down flux into and within the
262 folate network [10, 16, 20]. The proposed inhibitors in the *Rewired Model* also appear to
263 severely lower the amount of cellular DHF_n, which is achieved clinically by Sulfamethoxazole. This
264 means that the proposed set of inhibitors would be effective against some bacterial strains that
265 show resistance to TM and Sulfamethoxazole simultaneously. This is an unexpected but welcome

output of the *Rewired Model* which puts the poor SSE score in context and bolsters the result as a viable set of drug targets.

Conclusions

The current work presents a mathematical model of the *E. coli* folate network that improves on the previous effort in accuracy, scope, and applicability. A detailed look at TM's mechanism not only shows the importance of folate polyglutamation levels, but also of enzyme-metabolite interactions to overall dynamics of the folate cycle. The improved look at this well-studied system allows a programmatic drug target search for alternatives to both TM and Sulfamethoxazole. We present this approach as a radically more efficient method to dealing with antibiotic-resistant bacteria by building on past successes.

Acknowledgements

We thank Rick Dilling and Vivian Callier for their valuable comments.

References

1. Andersson, D.I. and D. Hughes, *Antibiotic resistance and its cost: is it possible to reverse resistance?* Nat Rev Micro, 2010. **8**(4): p. 260-271.
2. Stamm, L.V., *Global Challenge of Antibiotic-Resistant Treponema pallidum.* Antimicrobial Agents and Chemotherapy, 2010. **54**(2): p. 583-589.
3. Gandhi, N.R., et al., *Multidrug-resistant and extensively drug-resistant tuberculosis: a threat to global control of tuberculosis.* The Lancet. **375**(9728): p. 1830-1843.

4. El-Halfawy, O.M. and M.A. Valvano, *Chemical Communication of Antibiotic Resistance by a Highly Resistant Subpopulation of Bacterial Cells.* PLoS ONE, 2013. **8**(7): p. e68874.

5. Baccanari, D.P., et al., *Escherichia coli dihydrofolate reductase: isolation and characterization of two isozymes.* Biochemistry, 1977. **16**(16): p. 3566-3572.

6. Nijhout, H.F., et al., *A mathematical model of the folate cycle: new insights into folate homeostasis.* J Biol Chem, 2004. **279**(53): p. 55008-16.

7. Roje, S., *S-Adenosyl-l-methionine: Beyond the universal methyl group donor.* Phytochemistry, 2006. **67**(15): p. 1686-1698.

8. Miller, B.A. and E.B. Newman, *Control of serine transhydroxymethylase synthesis in Escherichia coli K12.* Canadian Journal of Microbiology, 1974. **20**(1): p. 41-47.

9. Greene, R.C. and C. Radovich, *Role of methionine in the regulation of serine hydroxymethyltransferase in Eschericia coli.* Journal of Bacteriology, 1975. **124**(1): p. 269-278.

10. Kwon, Y.K., et al., *A domino effect in antifolate drug action in Escherichia coli.* Nat Chem Biol, 2008. **4**(10): p. 602-608.

11. Kwon, Y.K., M.B. Higgins, and J.D. Rabinowitz, *Antifolate-induced depletion of intracellular glycine and purines inhibits thymineless death in E. coli.* ACS Chem Biol, 2010. **5**(8): p. 787-95.

12. Trimmer, E.E., et al., *Folate activation and catalysis in methylenetetrahydrofolate reductase from Escherichia coli: roles for aspartate 120 and glutamate 28.* Biochemistry, 2001. **40**(21): p. 6216-26.

13. McGuire, J.J., et al., *Enzymatic synthesis of folylpolyglutamates. Characterization of the reaction and its products.* Journal of Biological Chemistry, 1980. **255**(12): p. 5776-5788.

14. Shane, B., *Pteroylpoly(gamma-glutamate) synthesis by Corynebacterium species. Purification and properties of folypoly(gamma-glutamate) synthetase.* Journal of Biological Chemistry, 1980. **255**(12): p. 5655-5662.

15. Lee, J.C., et al., *The prevalence of trimethoprim-resistance-conferring dihydrofolate reductase genes in urinary isolates of Escherichia coli in Korea.* Journal of Antimicrobial Chemotherapy, 2001. **47**(5): p. 599-604.

16. Blahna, M.T., et al., *The role of horizontal gene transfer in the spread of trimethoprim–sulfamethoxazole resistance among uropathogenic Escherichia coli in Europe and Canada.* Journal of Antimicrobial Chemotherapy, 2006. **57**(4): p. 666-672.

17. Aflaki, E., et al., *Macrophage Models of Gaucher Disease for Evaluating Disease Pathogenesis and Candidate Drugs.* Science Translational Medicine, 2014. **6**(240): p. 240ra73.

18. Patnaik, S., et al., *Discovery, structure-activity relationship, and biological evaluation of noninhibitory small molecule chaperones of glucocerebrosidase.* J Med Chem, 2012. **55**(12): p. 5734-48.

19. Bonhoeffer, S., M. Lipsitch, and B.R. Levin, *Evaluating treatment protocols to prevent antibiotic resistance.* Proceedings of the National Academy of Sciences, 1997. **94**(22): p. 12106-12111.

20. Masters, P.A., et al., *TRimethoprim-sulfamethoxazole revisited.* Archives of Internal Medicine, 2003. **163**(4): p. 402-410.

21. Gangjee, A., et al., *Potent Dual Thymidylate Synthase and Dihydrofolate Reductase Inhibitors: Classical and Nonclassical 2-Amino-4-oxo-5-arylthio-substituted-6-methylthieno[2,3-d]pyrimidine Antifolates.* Journal of medicinal chemistry, 2008. **51**(18): p. 5789-5797.

22. Contestabile, R., et al., *l-Threonine aldolase, serine hydroxymethyltransferase and fungal alanine racemase. A subgroup of strictly related enzymes specialized for different functions.* Eur J Biochem, 2001. **268**(24): p. 6508-25.

23. Kisliuk, R., *Pteroylpolyglutamates.* Molecular and Cellular Biochemistry, 1981. **39**(1): p. 331-345.

24. Kisliuk, R.L., et al., *Polyglutamyl derivatives of tetrahydrofolate as substrates for Lactobacillus casei thymidylate synthase.* Biochemistry, 1981. **20**(4): p. 929-934.

25. Horiuchi, Y., et al., *Coupling effects of distal loops on structural stability and enzymatic activity of Escherichia coli dihydrofolate reductase revealed by deletion mutants.* Biochimica et Biophysica Acta (BBA) - Proteins and Proteomics, 2010. **1804**(4): p. 846-855.

26. Sheng, Y., et al., *Mutation of an essential glutamate residue in folylpolyglutamate synthetase and activation of the enzyme by pteroate binding.* Arch Biochem Biophys, 2002. **402**(1): p. 94-103.

27. Bognar, A., et al., *Folylpoly-gamma-glutamate synthetase-dihydrofolate synthetase. Cloning and high expression of the Escherichia coli folC gene and purification and properties of the gene product.* J Biol Chem, 1985. **260**: p. 5625 - 5630.

28. Bognar, A.L. and B. Shane, *[55] Bacterial folypoly([gamma]-glutamate) synthase-dihydrofolate synthase*, in *Methods in Enzymology*, D.B.M. Frank Chytil, Editor. 1986, Academic Press. p. 349-359.

29. Burton, E., J. Selhub, and W. Sakami, *The substrate specificity of 5-methyltetrahydropteroyltriglutamate-homocysteine methyltransferase*. Vol. 111. 1969. 793-795.

30. Whitfield, C.D., E.J. Steers, Jr., and H. Weissbach, *Purification and properties of 5-methyltetrahydropteroyltriglutamate-homocysteine transmethylase.* J Biol Chem, 1970. **245**(2): p. 390-401.

31. Trimmer, E.E., et al., *Aspartate 120 of Escherichia coli methylenetetrahydrofolate reductase: evidence for major roles in folate binding and catalysis and a minor role in flavin reactivity.* Biochemistry, 2005. **44**(18): p. 6809-22.

32. McGuire, J. and J. Bertino, *Enzymatic synthesis and function of folylpolyglutamates.* Molecular and Cellular Biochemistry, 1981. **38**(1): p. 19-48.

33. Mansouri, A., J.B. Decter, and R. Silber, *Studies on the regulation of one-carbon metabolism. II. Repression-derepression of serine hydroxymethyltransferase by methionine in Escherichia coli 113-3.* J Biol Chem, 1972. **247**(2): p. 348-52.

Supporting information

S1 Table. TM Model parameters.

S2 Table. SSE Outputs (observations vs simulations).

372 S3 Table. Experimental Data Replicates.

373 S1 Fig. Network Rewiring Reaction Velocities.

374 General flux in the system is lower than in the TM Model, and resultant fluxes over time differ
375 greatly from that of the TM Model.

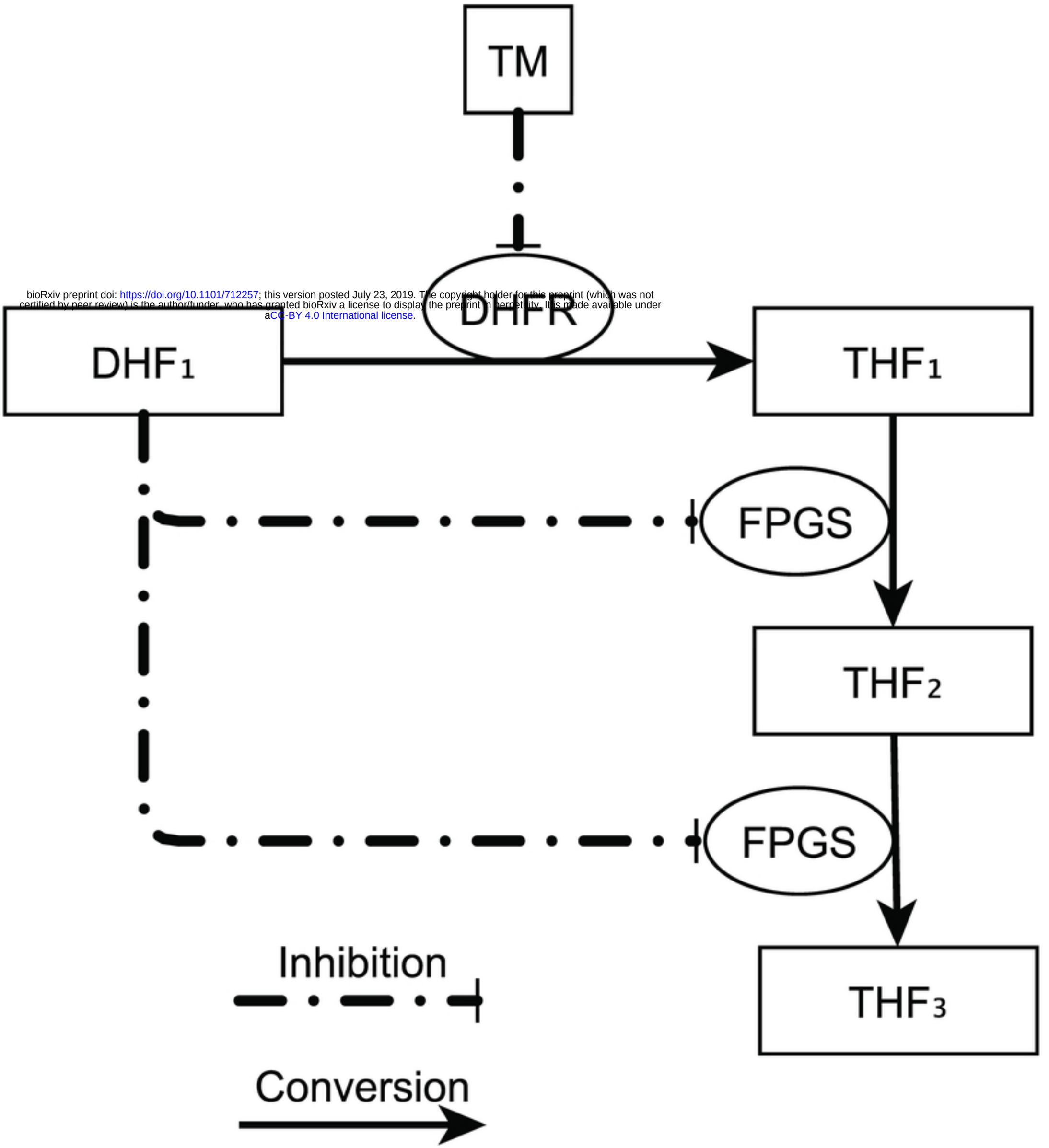

Figure

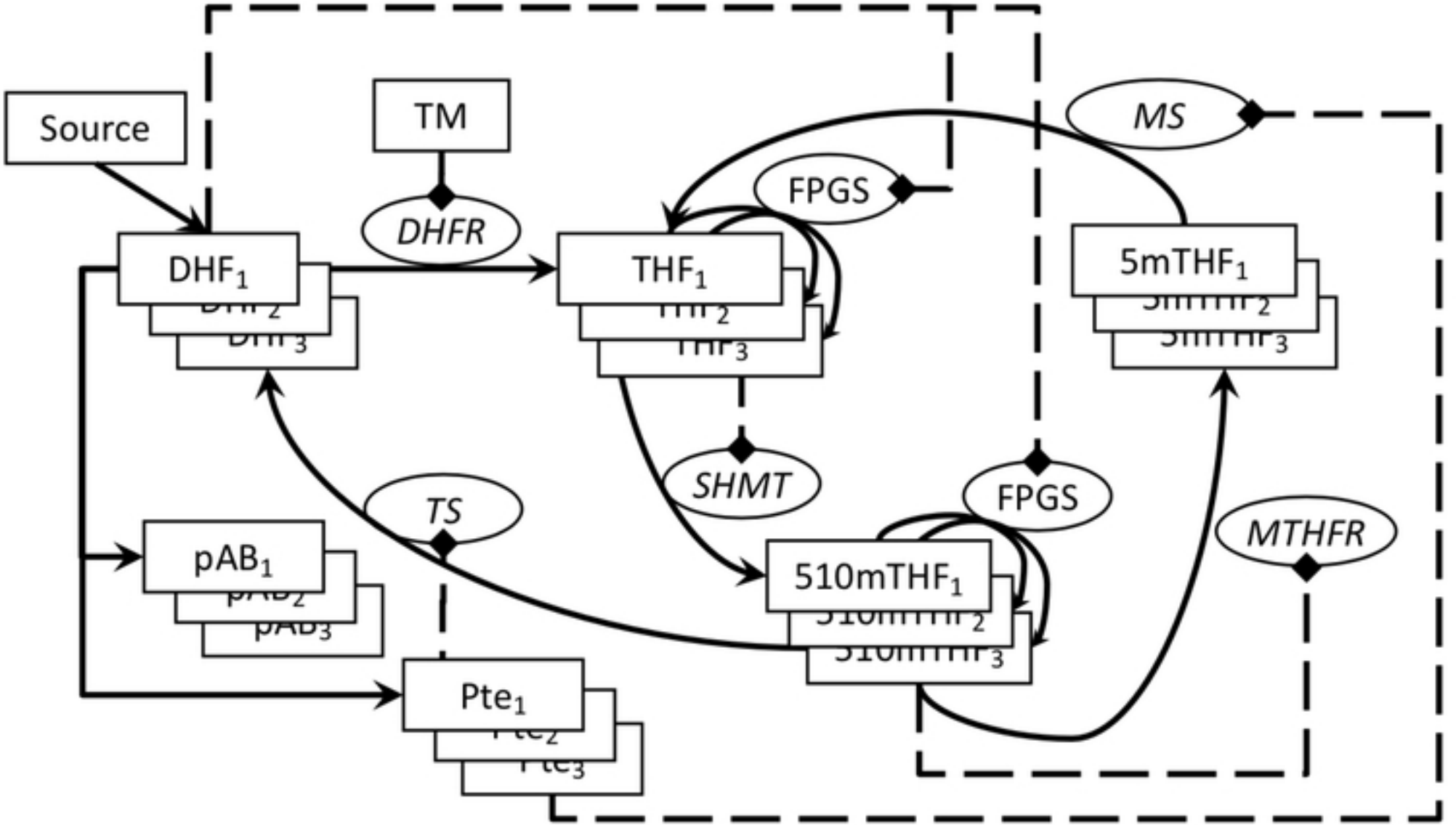
Source
TM
DHFR
DHF1
THF1
FPGS
MS
5mTHF1
SHMT
TS
FPGS
MTHFR
pAB1
510mTHF1
Pte1

Figure

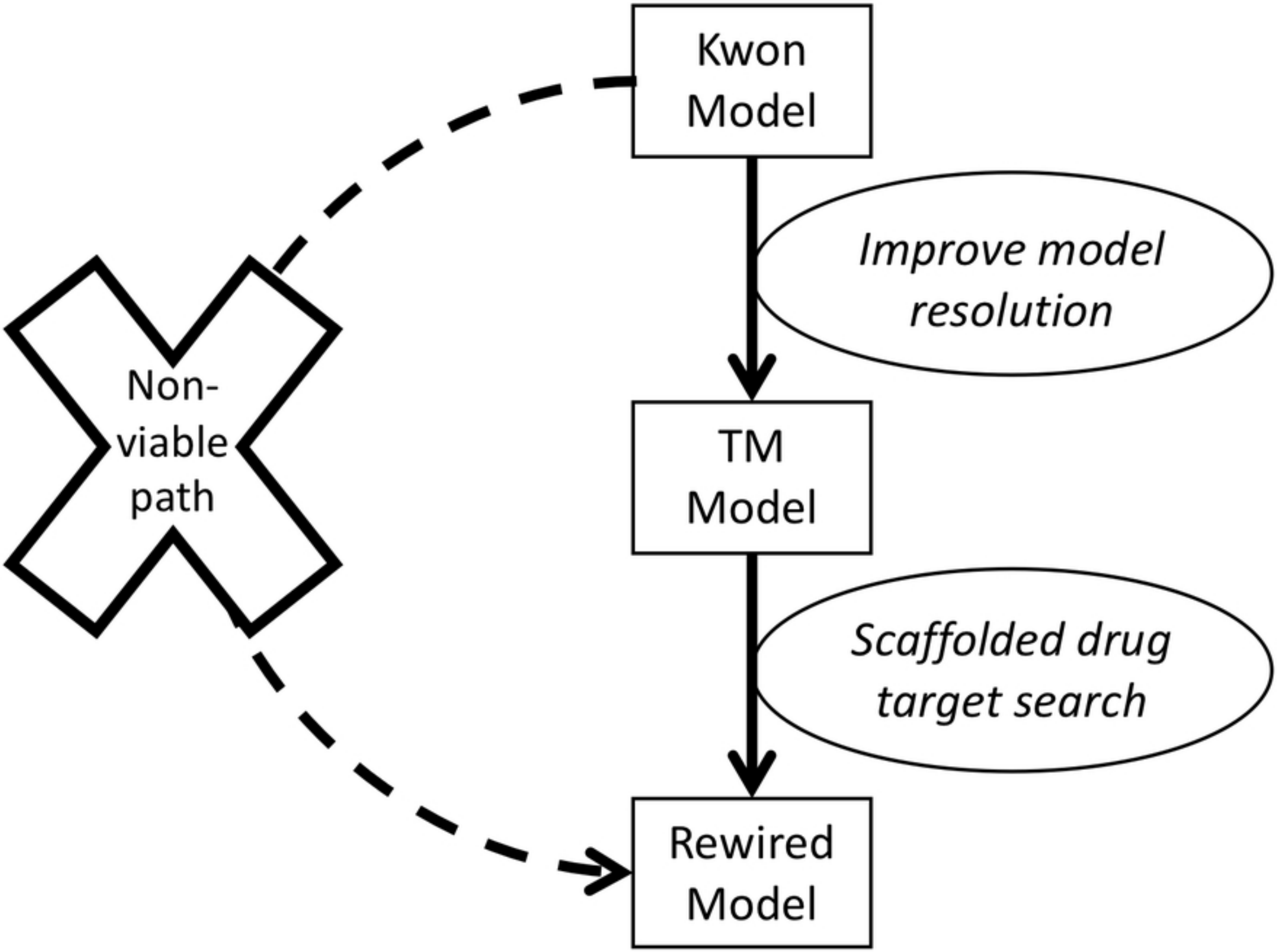
Kwon
Model
Improve model
resolution
Non-
viable
path
TM
Model
Scaffolded drug
target search
Rewired
Model

Figure

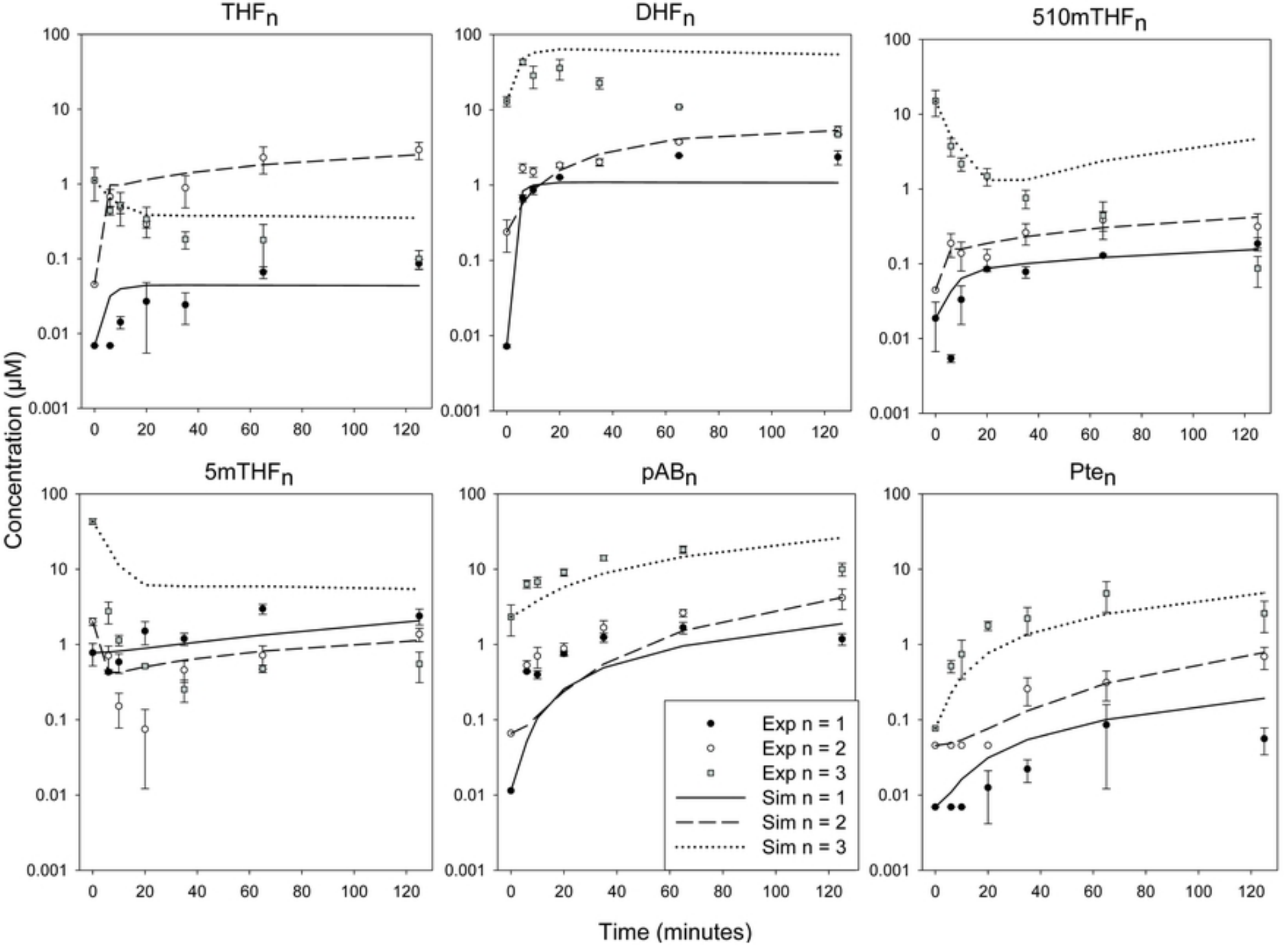
Trimethoprim Experimental and Simulated Metabolite Concentrations vs Time
THFn
DHFn
510mTHFn
5mTHFn
pABn
Pten
Concentration (μM)
Time (minutes)
Exp n = 1
Exp n = 2
Exp n = 3
Sim n = 1
Sim n = 2
Sim n = 3

Figure

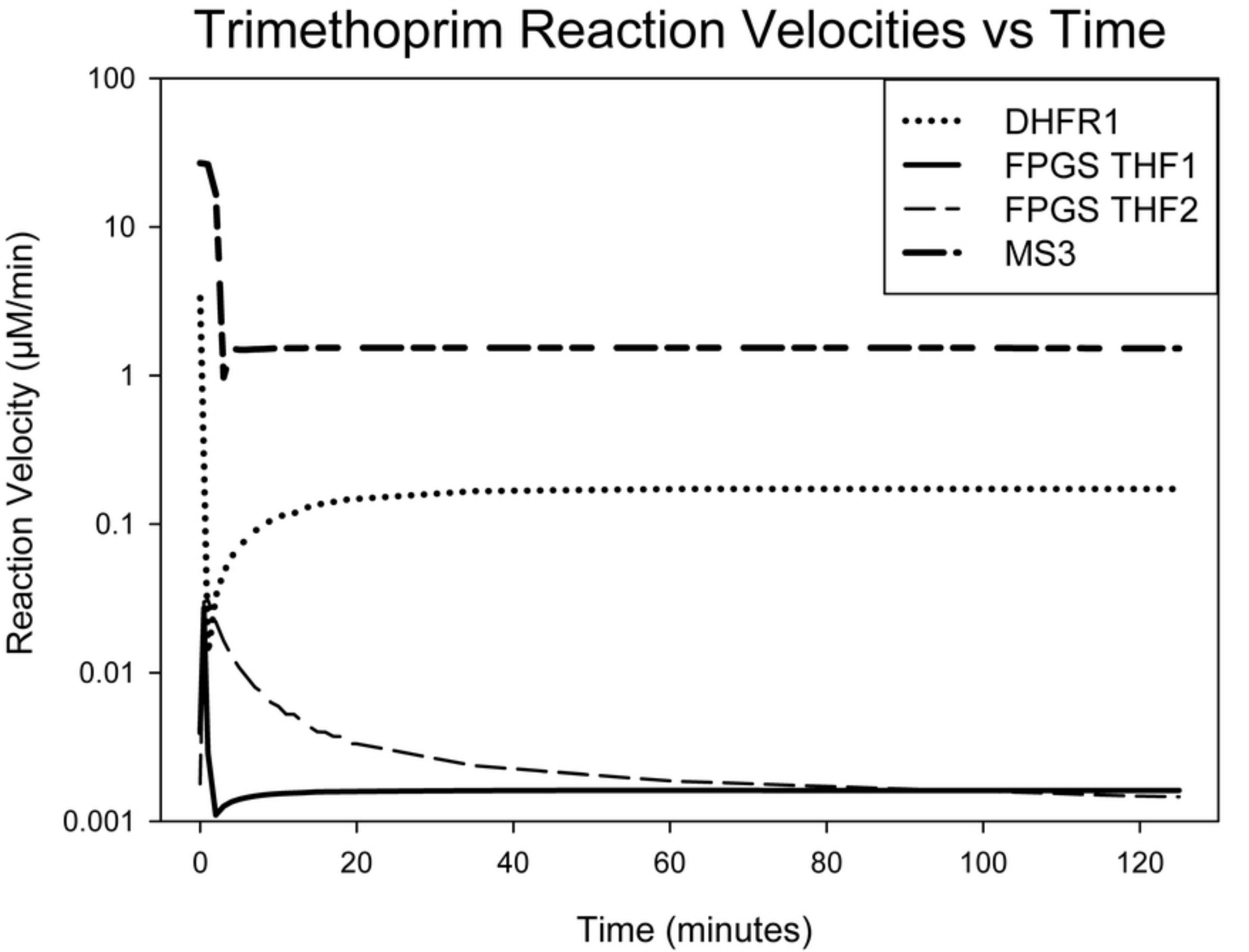
Trimethoprim Reaction Velocities vs Time
DHFR1
FPGS THF1
FPGS THF2
MS3
Reaction Velocity (μM/min)
100
10
1
0.1
0.01
0.001
0
20
40
60
80
100
120
Time (minutes)

Figure

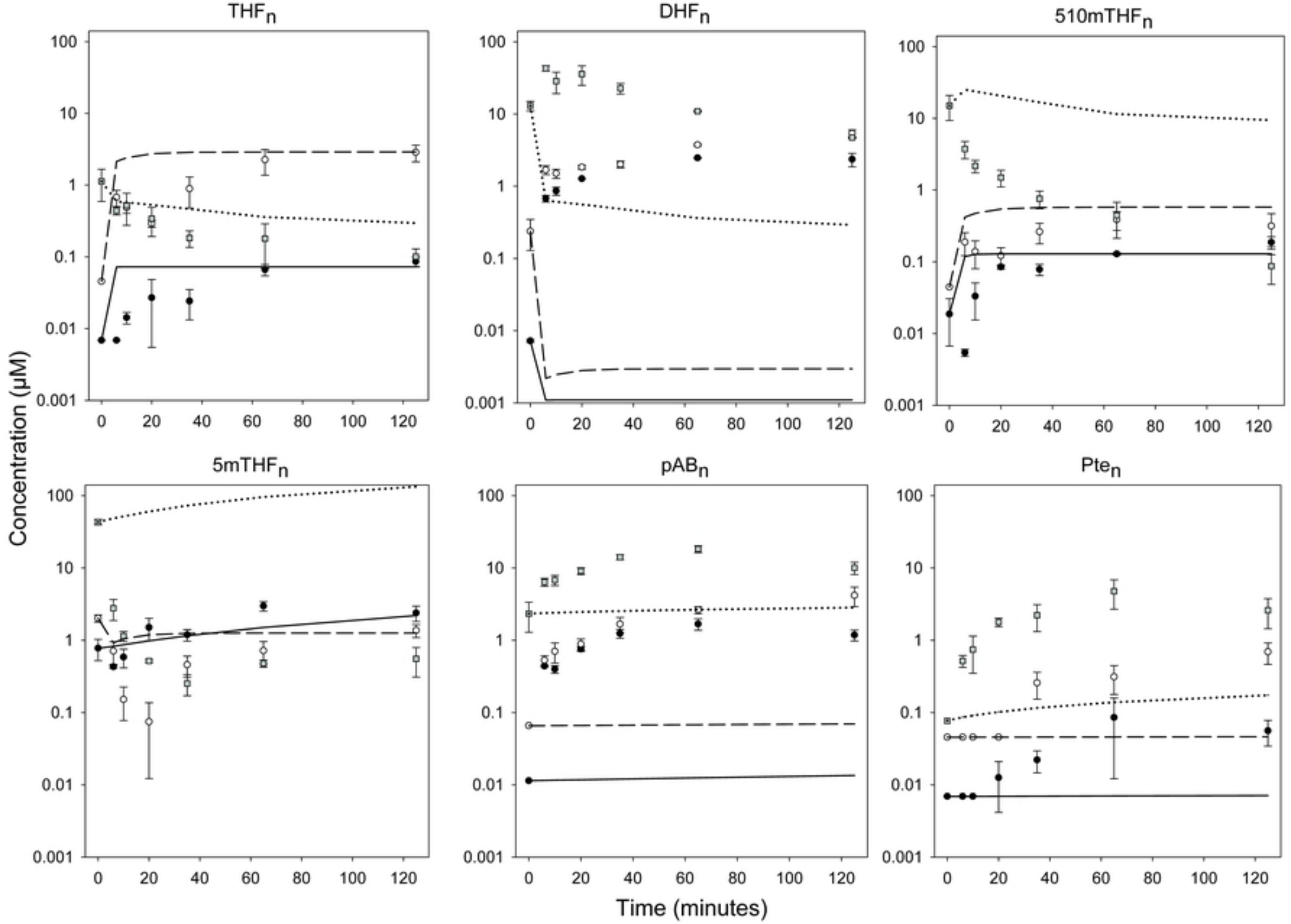
Rewired Experimental and Simulated Metabolite Concentrations vs Time
THFn
DHFn
510mTHFn
5mTHFn
pABn
Pten
Concentration (μM)
Time (minutes)
100
10
1
0.1
0.01
0.001
0
20
40
60
80
100
120

Figure